ADVANCES in NATURAL and APPLIED SCIENCES

ISSN: 1995-0772
EISSN: 1998-1090
2016November10(16):pages 17-29

Published BY**AENSI Publication**
http://www.aensiweb.com/ANAS
Open Access Journal

Intelligent Model to Approach the Finite-Element Solution of the Traveling Wave Induction Heating System

[1]Prof. Dr. A. K. Al-Shaikhli, [2]Asst. Prof. Dr. Abdul-Rahim T. Humod, [2]Fadhil A. Hasan (MSc)

[1]Dijlah University College, Baghdad, Iraq,
[2]Electrical Engineering Dep., University Of Technology, Baghdad, Iraq

Received 23 August 2016; Accepted 1 November 2016; Published 20 November 2016

Address For Correspondence:
Prof. Dr. A. K. Al-Shaikhli, Dijlah University College, Baghdad, Iraq,

Copyright © 2016 by authors and American-Eurasian Network for ScientificInformation (AENSI Publication).
This work is licensed under the Creative Commons Attribution International License (CC BY).http://creativecommons.org/licenses/by/4.0/

Open Access

ABSTRACT

Background: The finite-element analysis (FEA) is a universal method used to analyze traveling wave induction heating (TWIH) systems; Problem: the analysis procedure is extremely slow and requires long computation time. Objective: This paper proposed a novel intelligent model to represent the TWIH system. This model is based-on the artificial neural network (ANN), which is trained to approach the FE solution. Sets of training data patterns are obtained from the solutions of the FEA by using ANSYS program for specific cases. Results: Three degrees of freedom (magnetic field, eddy current densities and temperature) are obtained from the intelligent model. The time required for solution close to zero second with an acceptable percentage error in comparison with FEA. The performance of the proposed model is investigated by using MATLAB-SIMULINK. Conclusions: Results demonstrate the features of the proposed method from the high accuracy performance and fast analysis. Various study cases can be implementing, for different strip thickness and material type, in high flexible manner. Moreover, both of electromagnetic and thermal analysis can be combined in single analysis process which is very complicated problem in the FEA.

KEYWORDS: *Traveling wave induction heating, finite-element analysis, intelligent system.*

INTRODUCTION

In the last two decades the advantages of the Traveling Wave Induction Heating (TWIH) are proved in conjunction with their counterparts such as Transverse Flux Induction Heating (TFIH) and Ross Coil Induction Heating (RCIH) [1-3]. Many industrial applications for heating flat metals reckon on the features of the TWIH. A wide and uniform heat distribution, over the strip surface, can be achieved without needing to move the heater. Moreover, they not only profiteer the advantage of using line frequency, which reduces system's complexity and coast, but also represent balanced load to the power utility. In addition, they reduce the mechanical vibration of the heater and strip caused by the electromagnetic forces [2].

Generally, there are two main analysis methods; analytical and numerical methods. In the case of simple configuration systems the analytical method is particularly suitable. This method used on Fourier's series and Fourier's integral transformation for simple parametric analysis, and some simplifications and assumptions are essential [4]. In other hand, the numerical method is widespread and specifically useful for analyzing; the magnetic field, eddy current, power density and temperature distribution for complex geometry system, with considering; the edge-effect of both heater and strip, and slot effect which are very important in TWIH analysis. The available 2-D and 3-D finite-element analysis (FEA) programming code can be used for any geometry [5]. In this method an advance known of the excitation current can obtains multi degrees of freedom (DOF) such as; coil EMF, magnetic field density, eddy current density, electromagnetic forces, and temperature distribution.

To Cite This Article: Prof. Dr. A. K. Al-Shaikhli, Asst. Prof. Dr. Abdul-Rahim T. Humod, Fadhil A. Hasan (MSc)., Differential EvolutionaryAlgorithm Based MPPT Controlled Inverter for Solar PV Led Street Light Systems. **Advances in Natural and Applied Sciences**. 10(16);Pages: 17-29

The nonlinearity of the magnetic core can be also taken into account due to analysis processing. However, the complicated geometries of complex electromagnetic field problems lead to large number of discrete nodes and consequently to a huge computational efforts [6]. As an example, for acceptable accuracy performance a 0.01ms time step is sufficient in transient analysis, so by observations technique, it is required a few days to achieve total analysis of 3-D finite-element method. Certainly, this very long computation time is impractical for engineering applications [7].

With recent advances in artificial intelligence, genetic algorithms, and neural networks, several attempts have been proposed to reduce the FEA computation time in TFIH design by using intelligent systems [8]. But, in the TWIH analysis there has not been applicable approaches to reduce computation time except single attempt to apply a method that combined a neural network with FEA to the design of a TWIH system to offset the resulting inhomogeneous eddy current or power density [9].

This paper proposed a novel method to estimate three main DOFs of the TWIH finite-element solution based on three stages neural networks. A multi-objective intelligent model is designed and trained to predict three DOFs; magnetic field density, eddy current density and temperature distribution according to the knowledge of; supply voltage, ambient conditions, strip's thickness and conductivity. The accuracy performance and features of the proposed intelligent model are demonstrated. Also, the production of the eddy current density and temperature distribution are examined in conjunction with the FE solution. Moreover, the influence of load material type and thickness has been analyzed for different operation conditions.

Configuration of TWIH system:

The schematic configuration of typical TWIH system is shown in fig. 1, it consist of two linear inductors with three-phase exciting current carried by conductors located on the opposite side of the strip and perpendicular to the direction of its movement [10]. As be seen, the carrying conductors located inside the slots of two magnetic yokes. The winding arrangements could affect the results of 3-D simulation and the choice of a suitable power supply and heat distribution as the strip surface.

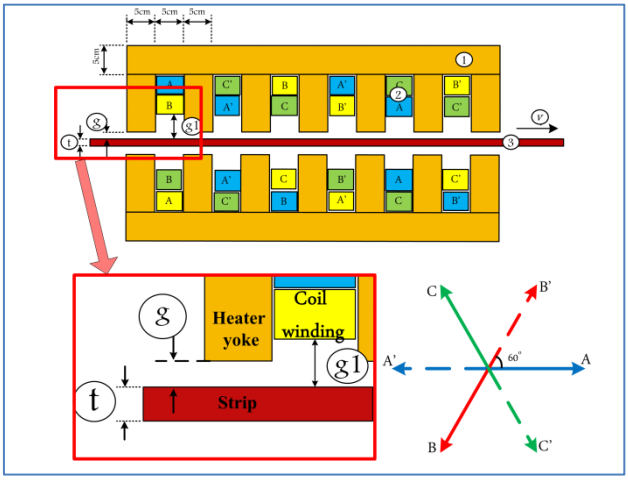

Fig. 1: System configuration

Researches demonstrated that the wide and uniform heat range and higher heating time can be achieved with short-pitch coil and up-down mode more than full-pitch and left-right coil arrangement [11]. Therefore, in this work the short-pitch and up-down winding arrangement is used and they are excited by three-phase current of 120° phase shift apart and 50Hz frequency. The air-gap between the inductor and the strip (g) is relatively large due to the thickness of the interposing refractory material.

System analysis:

The mathematical model of the electromagnetic phenomena is based on Maxwell's equations and wave propagation theory; the four equations are as the following:

$$\nabla\times\overline{H} = \overline{J} + \partial\overline{D}/\partial t \quad (1)$$

$$\nabla.\overline{B} = 0 \quad (2)$$

$$\nabla\times\overline{E} = -(\partial\overline{B}/\partial t) \quad (3)$$

$$\nabla.\overline{D} = \rho \quad (4)$$

Where: $\overline{H}$ is the magnetic field intensity, $\overline{B}$ is the magnetic field density, $\overline{E}$ is the electric field intensity, $\overline{D}$ is the electric displacement vector, and $\overline{J}$ is the current density, ρ is volume charge density.

Since $\bar{D} = \varepsilon\bar{E}$ and $\bar{J} = \sigma\bar{E}$ where: ε is the permittivity, σ is the conductivity.

Rewrite (1):

$$\nabla\times\bar{H} = \sigma\bar{E} + \varepsilon(\partial\bar{E}/\partial t) \quad (5)$$

For sinusoidal magnetic field:

$$\nabla\times\bar{H} = (\sigma + j\varepsilon\omega)\bar{E} \quad (6)$$

For super conducting materials:

$$\sigma \gg \varepsilon\omega \quad \rightarrow \quad \nabla\times\bar{H} = \sigma\bar{E} = \bar{J}$$

Since $\bar{B} = \nabla\times\bar{A}$ where $\bar{A}$ is the magnetic vector potential, then the mathematical model of the eddy current results can be described by means of the complex magnetic vector potential $\bar{A}$ and a complex scalar potential φ (where φ is the magnetic scalar potential H= -∇φ):

$$\bar{J} = -\sigma(\partial\bar{A}/\partial t + \nabla\,\partial\bar{\varphi}/\partial t) + \bar{J}_s \quad (7)$$

Where: $\bar{J}_s$ is the impressed exciting current density.

It can be seen from (7) that the current density in the strip is proportional to the rate of change of the magnetic flux and the field intensity, so magnetic field which is inducted by TWIH can create different vortex effect in the strip [12].

Finite-element analysis:

In this paper the FE analysis has been performed by using ANSYS program, in which the FEA code is called as an external subroutine. The 3-D ANSYS theoretical model is shown in fig. 2.

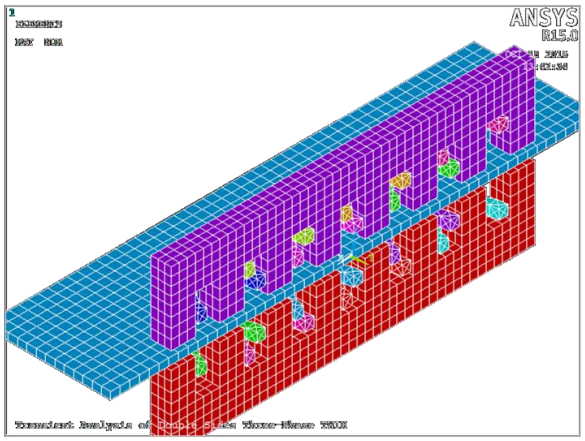

Fig. 2: A one-half symmetry 3-D FEA (ANSYS) model

The selected element type of the model materials is 'solid 236', which is a 3-D 20-node element capable of modeling electromagnetic fields. This element has magnetic and electric degrees of freedom. Magnetic DOFs are based on the edge-flux formulation. The edge-flux (Az) DOF are the line integrals of the magnetic vector potential along the element edges. The geometry, nodes location, faces and the coordinate system, for the 'solid 236' element, are shown in fig. 3.

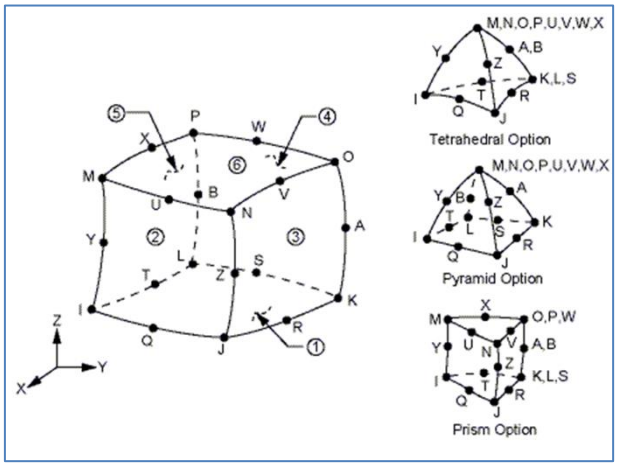

Fig. 3: Geometry of 'solid 236' element

The nonlinearity of the iron core is taken into account by using the B-H relationship parameter. After the materials are defined, applied voltage is specified to the coil, and VOLT constraint is coupled on the strip. Then parallel flux and normal flux boundary condition is added, finally calculations based on FEA is done by the transient analysis solving routine. System parameters, which are used in the simulation model, are summarized in table 1:

Heater	Length	0.65m
	Height	0.15 m
	Width	0.25 m
	Relative Permeability	Steel B-H curve
	No. of phases	3
	Excited phase voltage	50-200, step 50V
	Frequency	50 Hz
	Air gap	10 mm
Strip (Aluminum)	Length	1.5 m
	Width	0.5 m
	Thickness	1, 5, 10 and 15mm
	Resistivity (ρ)	2.86×10^{-8} Ω.m
	Relative Permeability	1 (Dimensionless)
	Movement velocity	1 m/min
Thermal conditions	Ambient temperature	25 C^o
	Convection coefficient	100 W/(m^2.C)
	Thermal conductivity	211 W/(m.C)

Figs. 4-6 show the solution of magnetic field density, eddy current density and temperature distribution respectively for certain study case of; 100V input voltage, conductivity=3.5×10^7 S/m (aluminum), thickness=10mm, and 25^o ambient temperature.

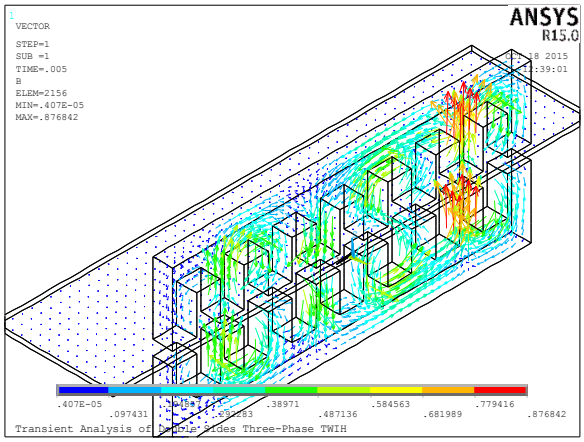

Fig. 4: Magnetic field density at angle 270^o (one-half symmetry)

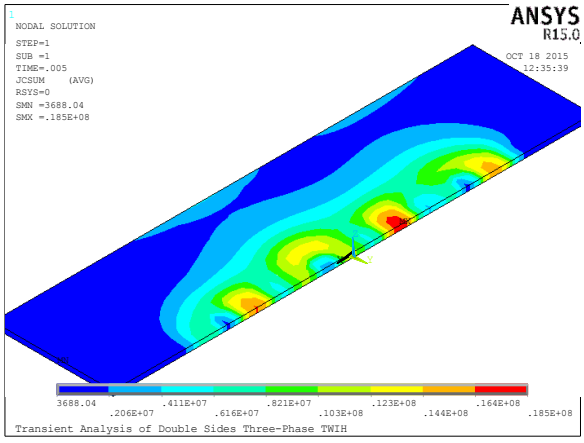

Fig. 5: Eddy current density (one-half symmetry)

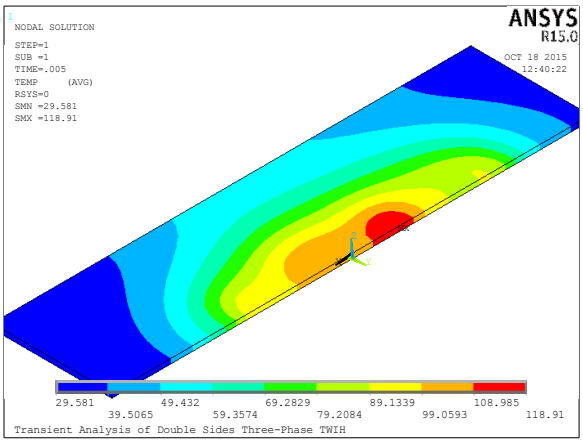

Fig. 6: Temperature distribution (one-half symmetry)

Artificial neural model:

The energy transfers, in the TWIH system from input to output, through three stages; electric-to-magnetic, magnetic-to-eddy current, eddy current-to-heat as shown in fig. 7. In this work these three stages will be replaced by three independent artificial neural networks (ANNs) [7].

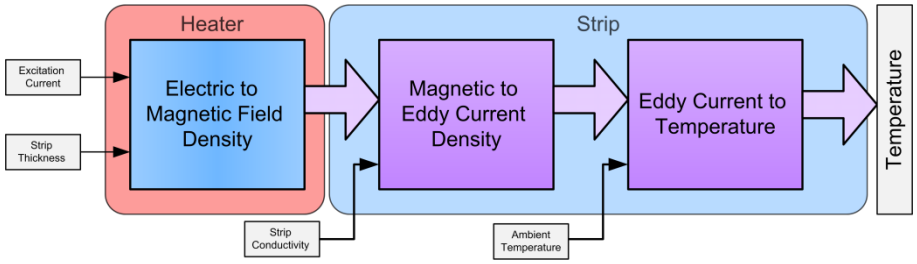

Fig. 7: Flow diagram for energy transferred in TWIH

The first stage transfers electric energy, acted by the excitation current, to magnetic energy which acted by the magnetic field density. The produced magnetic field density depends on the applied voltage and the design parameters of the inductor such as; Configuration of the heater yoke, winding arrangements and number of turns air-gap between the heater and strip surface, poles cross-section area and strip thickness.

In this work the proposed artificial model is designed for a specific TW inductor of fixed configuration and parameters (i.e. points i to iv above), and they are taken as same as the configuration and parameters of the FE model. Therefore, the only dependant variables are the applied voltage and strip thickness, which are to be the inputs of the first ANN. In the other side the ANN has eight outputs, each one of them represents the average value of the magnetic field density over the cross-section area of one from eight poles in the magnetic yoke. The FE solution of this system tabulates the input-output training data of the magnetic field density predictive ANN. The training data sets obtained from the variation of both the applied voltage by: 50, 100, 150, and 200V and the strip thickness by: 1, 5, 10, and 15mm. Fig. 8 shows structure the magnetic ANN which has seven hidden layers, two inputs and eight outputs.

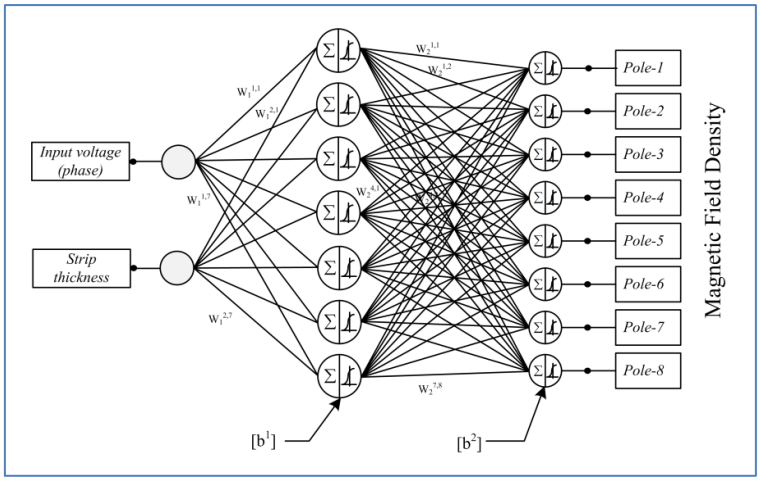

Fig. 8: The structure of the magnetic field ANN

The second ANN is the magnetic field-to-eddy current energy conversion stage. This network demonstrates the magnitude value of the eddy current density distribution over a selected area from the strip's surface. An area of 100x25cm^2 is selected below the heater face and divided into 306 brick elements (according to the nodes number), which represents a discrete evaluation of the eddy current density distribution over the strip's surface. In order to increase the accuracy and reduce training time it's preferred to reduce the number of outputs. Therefore, the selected area is divided into 9 longitudinal slices, each slice has 34 elements. Hence, the ANN is designed to be a combination of three subnets; each subnet has 102 outputs represent three of the nine slices from the selected area. Since, the amount of the induced eddy current depends on the produced magnetic field and the conductivity of the strip's material. Therefore, each subnet has nine inputs; the eight magnetic field density predicted by previous magnetic ANN, and the ninth input is the conductivity value of the strip's material. The FE solution for different applied voltage, strip's thickness, and conductivity is tabulating the training data of the neural network. The conductivities of five materials (lead, brass, aluminum, copper and silver) are used to obtain the training data, it's important to indicate here; in order to training the ANN for wide range of metals the highest conductivity metal (silver) is used, which may be unsophisticated practical application for this size of the metal. The structure of one subnet of the eddy current ANN can be shown in fig. 9 which has five hidden layers, nine inputs, and 102 outputs:

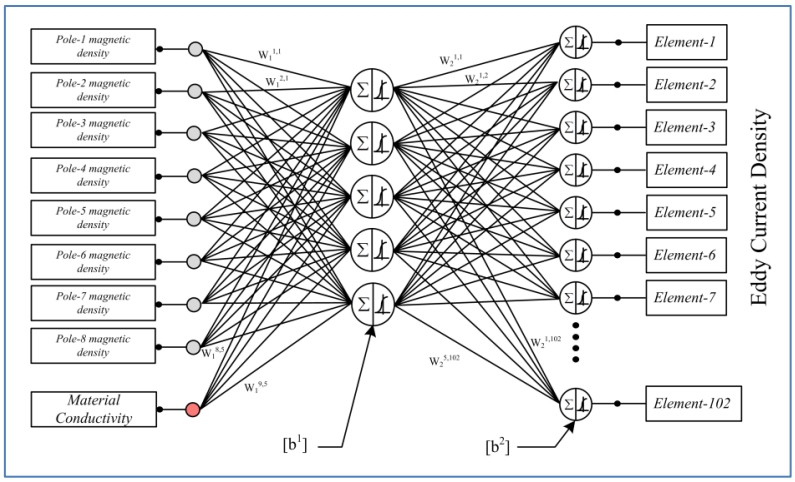

Fig. 9: the structure of one of three of the eddy current ANN

The third stage of energy conversion is the temperature production stage, in which the induced eddy current produces heat energy due to power dissipated within the strip material. The amount of the produced temperature and its rising time depend on the conductivity and thickness of the material, and the surrounded condition such as: ambient temperature, thermal conductivity, and convection coefficient. Since, the effects of material thickness and conductivity are taken in account previously in the first and second ANNs. Then, only the surrounded condition is the dominant effective factors, in this work the thermal conductivity and convection coefficient are assumed to be constant and the dependent variable is only the ambient temperature.

There are two methods for selecting the inputs of the ANN: first is to use the eddy current density predict by the second ANN which requires 306 inputs equal to the number of strip elements. And second is using the magnetic field density predicts by the first ANN which requires eight inputs equal to the poles number. In order to reducing the complexity and the training time the second method is selected. The strip surface divided into 312 elements (according to the element numbers) with 13 slices, each slice has 24 elements. In order to reduce the number of output elements (to reduce complexity and computation time) a new strategy is used by using the odd number of the surface elements only. Therefore, the numbers of outputs are: 156 element, 13 slices, and 12 elements/slice. Hence, the temperature ANN stage is represented by single neural network has nine inputs include the eight magnetic field density plus the value of the ambient temperature, while it has 156 outputs of 13 slices. The training data is obtained from the FE solution for various applied voltage, strip thickness, material conductivity, and ambient temperature from 0º to 50º by step 10º. Fig. 10 shows the structure of the temperature ANN which has six hidden layers, nine inputs, and 156 outputs:

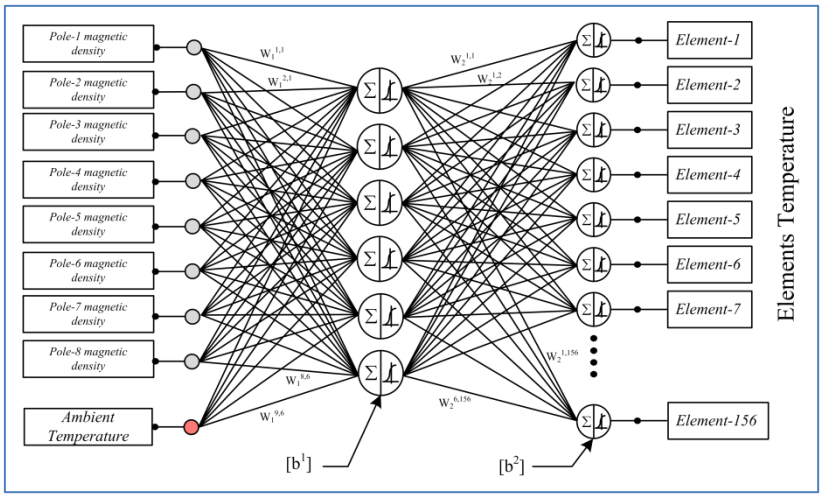

Fig. 10: The structure of the temperature ANN

The accuracy performances of the three ANNs are depicted in figs. 11-13 for study case of: study case of; 200V input voltage, conductivity=6.1x10^7 S/m (silver), thickness=5mm, and 25º ambient temperature.

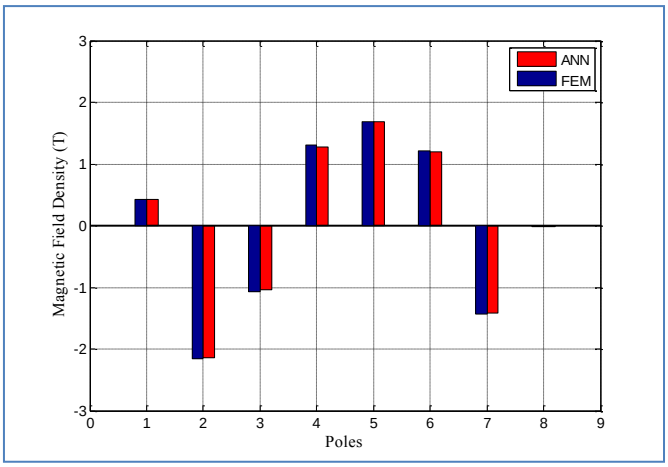

Fig. 11: Accuracy performance of the magnetic ANN

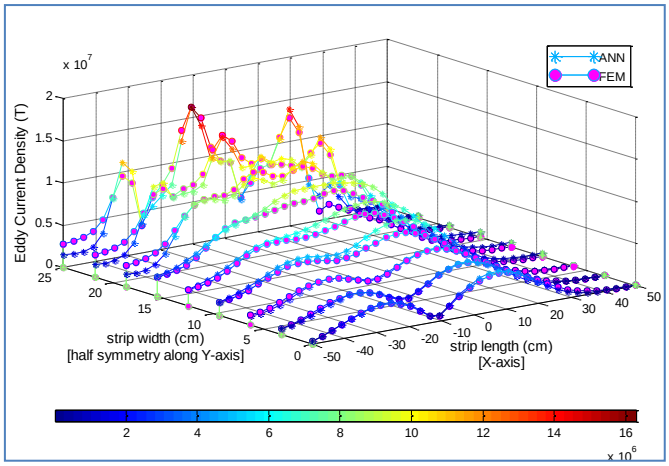

Fig. 12: Accuracy performance of the eddy current ANN (one-half symmetry)

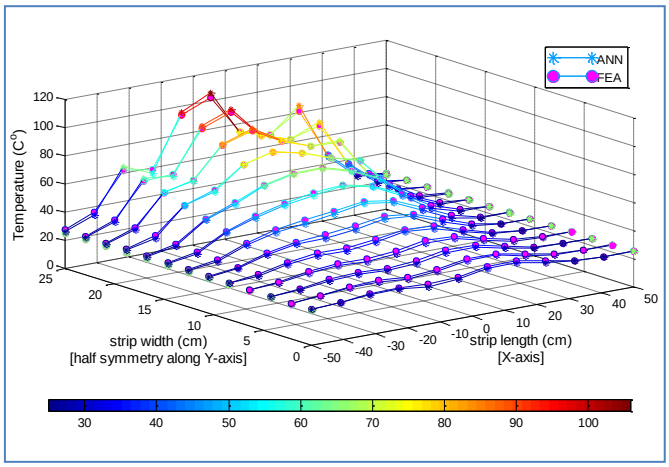

Fig. 13: Accuracy performance of the temperature ANN (one-half symmetry)

Simulation results:

The overall artificial neural model can be simulated by using MATLAB-SIMULINK, the three artificial neural networks and their subnets can be collected in single simulation as shown in fig. 14. The overall intelligent model has four nested inputs distribute over the three networks as previously explained, these four inputs are; the magnitude of applied phase voltage, the strip thickness, the strip material conductivity, and the ambient temperature.

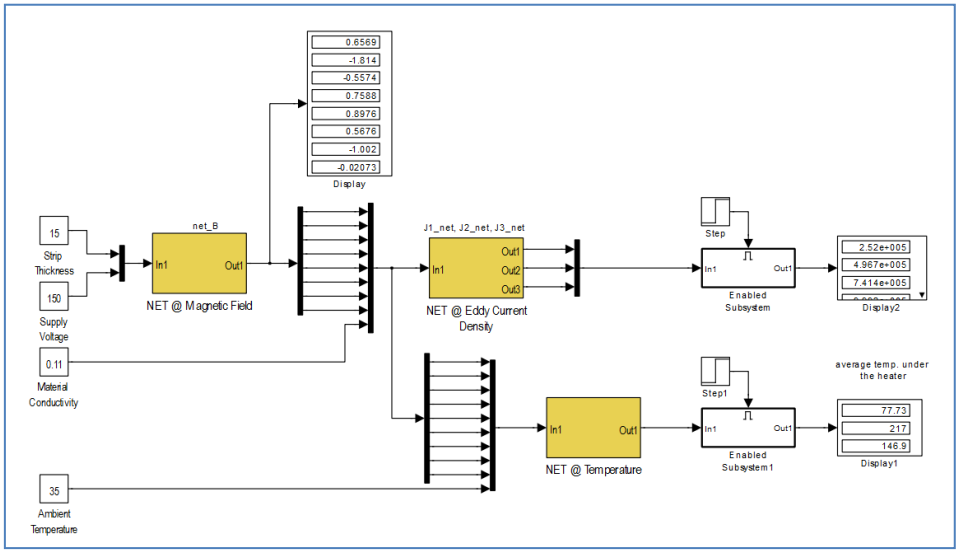

Fig. 14: The overall ANN model simulation

The ranges of these inputs are limited within the range of the training data; V_{in}=50-200V, thickness=1-15mm, conductivity=$5x10^6$ (lead)-$0.61x10^8$ (silver), ambient temperature=0^o-50^o. In other side, the intelligent model has three separate outputs groups; the first group is the magnetic field density which has eight outputs, the second group is the eddy current density which has 306 outputs, and the third group is the temperature distribution which has 312 outputs. For comparison purposes the performance of the proposed intelligent model and the FEA solution can be shown in figs. 15-18 , the eddy current density and temperature distributions are illustrated for two different operation cases; (applied voltage=150V, strip thickness=15mm, conductivity=$0.11x10^8$ (brass), ambient temperature=35^o), and (applied voltage=180V, strip thickness=3mm, conductivity=$0.58x10^8$ (copper), ambient temperature=15^o). Moreover, fig. 19 shows a comparison investigation between the FE solution and the proposed method for different strip materials due to the variation of applied voltage; (50, 75, 100,125,150,175, and 200V), the selected materials are: lead, aluminum, copper, and silver.

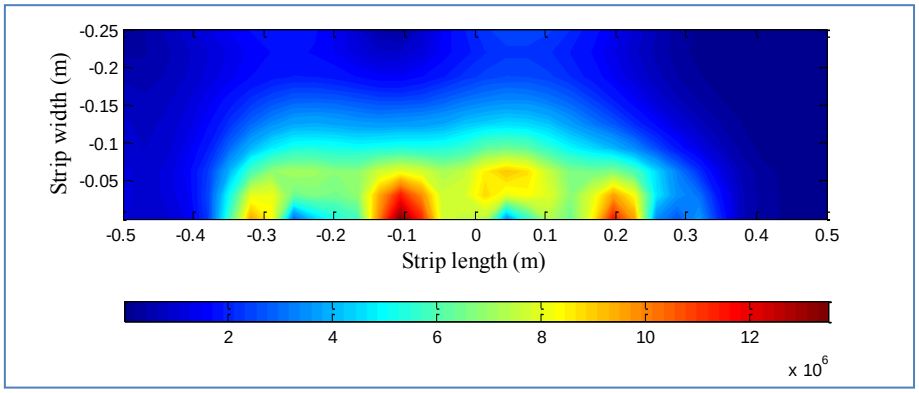

(a)

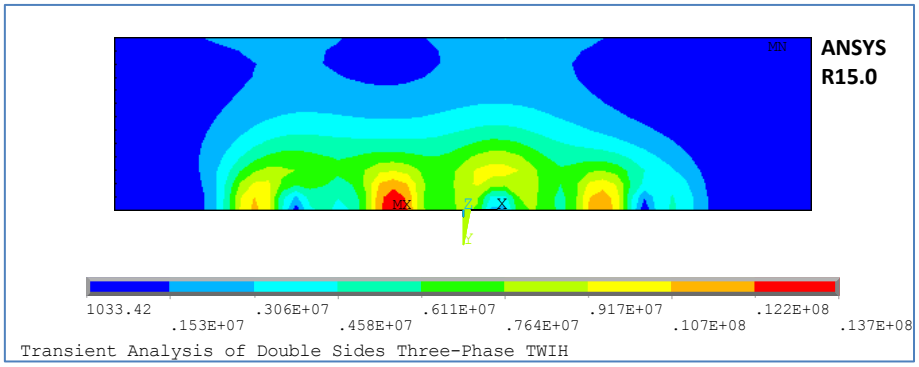

(b)

Fig. 15: The eddy current distribution for case-1 (one-half symmetry), a) ANN model, b) FEA simulation

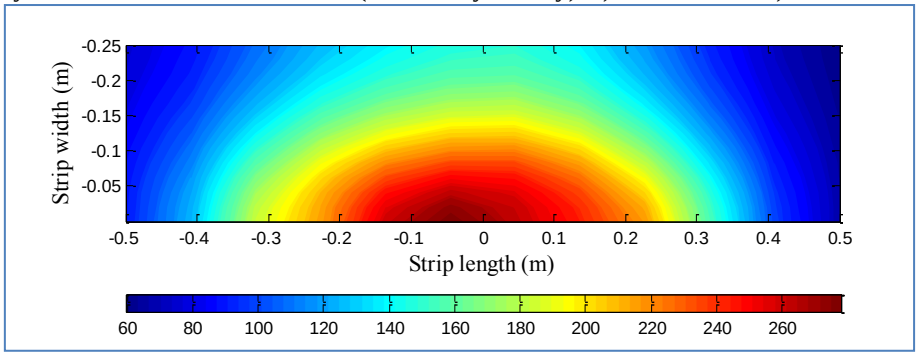

(a)

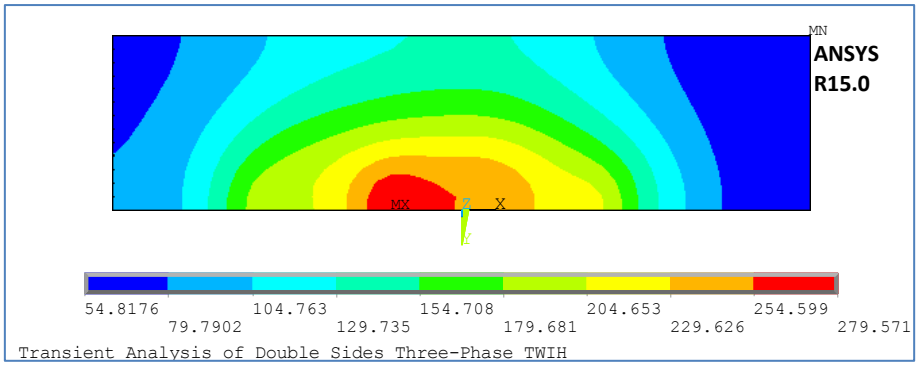

(b)

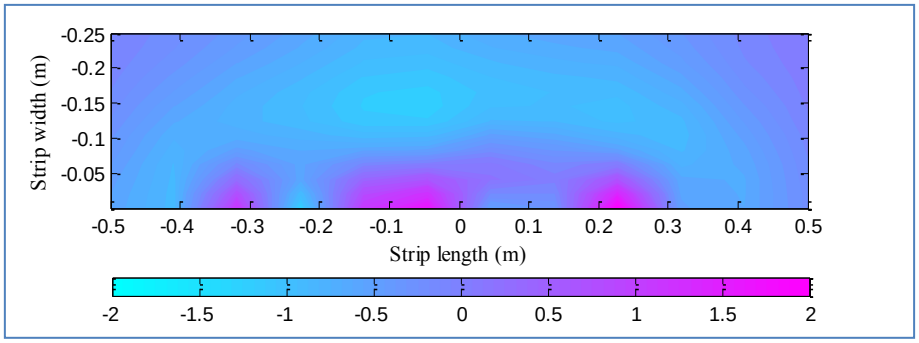

(c)

Fig. 16: Temperature distribution for case-1 (one-half symmetry), a) ANN model, b) FEA simulation, c) temperature error C^{o}

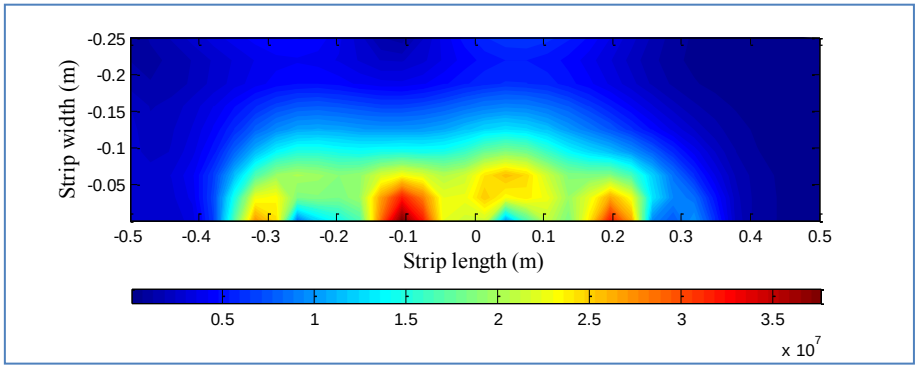

(a)

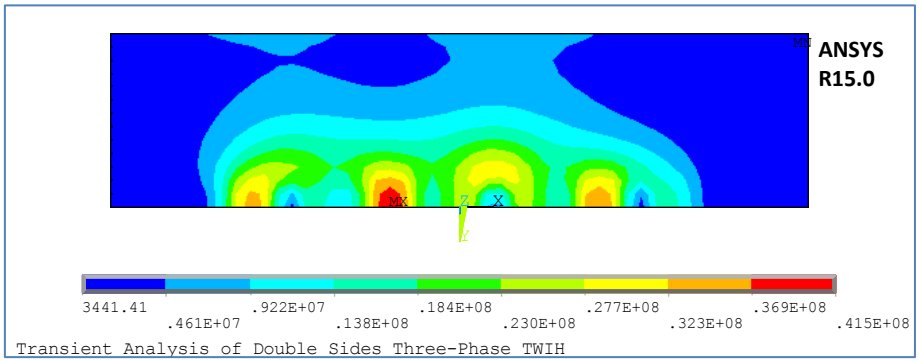

(b)

Fig. 17: eddy current distribution for case-2 (one-half symmetry), a) ANN model, b) FEA simulation

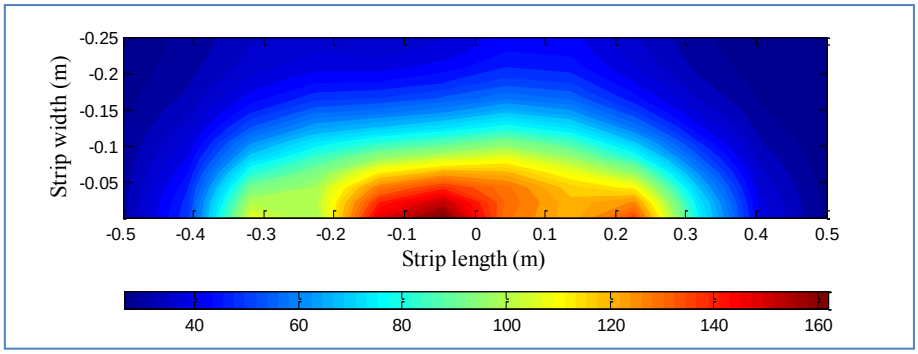

(a)

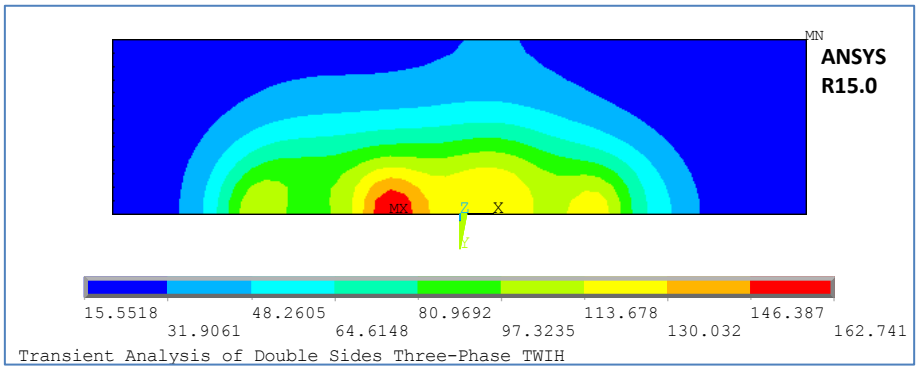

(b)

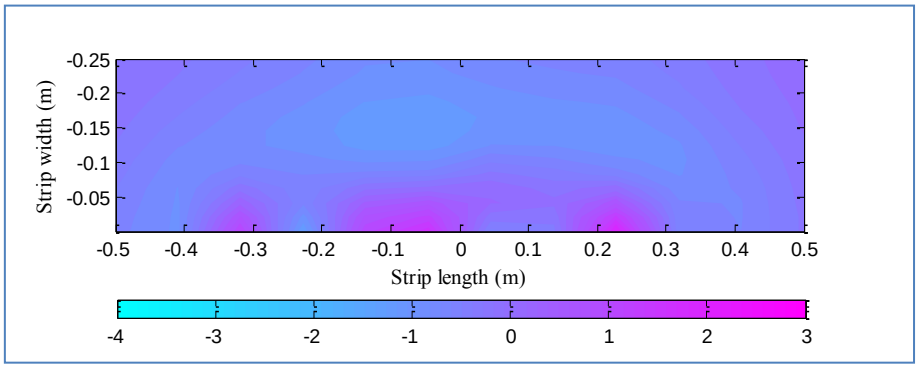

(c)

Fig. 18: temperature distribution for case-2 (one-half symmetry), a) ANN model, b) FEA simulation, c) temperature error C^{o}

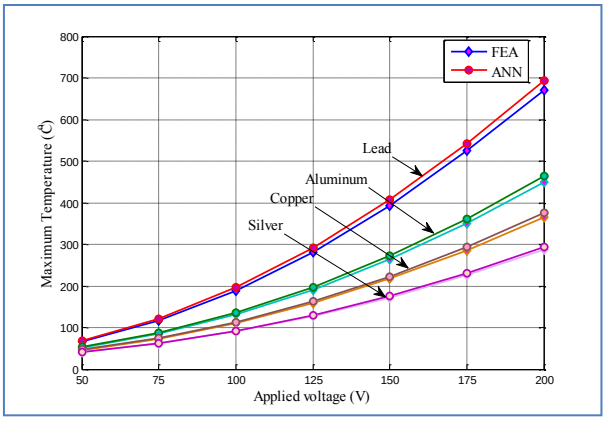

Fig. 19: maximum temperature due to applied voltage variation

Obviously, from the first moment anybody who has experience in the field of finite-element simulation and analysis software can realize the advantage of the proposed intelligent model from the immediately obtaining

solution and the high flexibility of parameter variation with an acceptable accuracy performance. Tables 1, 2 demonstrate the features of the proposed method by comparison between its performance and the FE-ANSYS solution for different operation conditions. Clearly, results show an excellent approach to the FE solution, with an acceptable percentage error especially within the heating region as compared with [2 and 6]. The big profit of reducing the computation time may lead to overlook the simple error margin in the performance of the proposed ANN model.

Table 1:

10mm thickness, 100V applied voltage	Maximum temperature C°								
	Ambient temp. 5°			Ambient temp. 25°			Ambient temp. 45°		
	ANN	FEA	%error	ANN	FEA	%error	ANN	FEA	%error
Lead	172.1	169.2	1.7139	194.1	189	2.6984	216.1	209	3.3971
Brass	158.9	159.4	0.3137	178.9	179.4	0.2787	199	199.4	0.2006
Aluminum	98.4	101.5	3.0542	126.7	131.5	3.6502	137.3	151.5	2.7723
Copper	69.5	73	4.7945	89.8	92.9	3.3369	109.5	112.9	3.0115
Silver	68.3	70.6	3.2578	88.2	90.6	2.6490	108.1	110.6	2.2604

Table 2:

100V applied voltage, 25C° ambient	Maximum temperature C°								
	Strip thickness 5mm			Strip thickness 10mm			Strip thickness 15mm		
	ANN	FEA	%error	ANN	FEA	%error	ANN	FEA	%error
Lead	228	230.9	1.2560	196.1	189.8	3.3193	154	153.5	0.3257
Brass	259.8	263	1.2167	178.9	179.4	0.2787	133.9	133.7	0.1496
Aluminum	219	227	3.5242	127.3	131.5	3.1939	92.4	93.4	1.0707
Copper	168	169.5	0.8850	89.7	92.9	3.4446	65.2	66.7	2.2489
Silver	164.5	165.4	0.5441	88.6	90.6	2.2075	64.1	65.1	1.5361

Conclusions:

Clearly, the proposed intelligent model in this paper gives an excellent performance in conjunction with the conventional finite-element analysis. The intelligent model approaches the finite-element (ANSYS) solution with an acceptable percentage error for different variation in the strip thickness and material type. The salient feature of the proposed method is the (approximately) zero computation time and flexibility of variables variation. Moreover, this intelligent model has the ability to combine the electromagnetic analysis with the thermal analysis in single simulation, which is a complicated process in FEA. This method is extremely convenient for performance studying and analysis the response to disturbances or parameters variation. As mentioned before, any one has experience in the field of electromagnetic analysis can realize from the first moment the difference between the proposed method and FEM. The drawback of this method is that; the intelligent model designed for a specific TWIH system configuration and hence any variation in system configuration requires a new model.

REFERENCES

1. Ali, V., F. Bukanin, S. Dughiero, Lupi, and V. Nemkov et al., 1994. “Simulation of Multiphase Induction Heating Systems,” in IEE Conference Publication, 38(4): 211-214.
2. Ali K. Al-shaikhli, Abdul-Rahim T. Humod, Fadhil Abbas, 2016. "Five-phase travelling wave induction heater for continuous heating of flat material", IET the Journal of Engineering, pp: 32, DOI: 10.1049/joe.2015.0145.
3. Wang Youhua, Wang Junhua, Li Jiangui, Li Haohua, 2008."Analysis of induction heating eddy current distribution based on 3D FEM," Computational Technologies in Electrical and Electronics Engineering, 2008. IEEE Region 8 International Conference on, pp: 238-241.
4. Junhua Wang, Youhua Wang,Ho, S.L. Xiaoguang Yang, Fu, W.N. Guizhi Xu, 2011. "Design and FEM Analysis of a New Distributed Vernier Traveling Wave Induction Heater for Heating Moving Thin Strips," IEEE Transactions on Magnetic, 47(10): 2612-2615.
5. Kenneth Frogner, Tord Cedell, 2014. Mats Andersson "Decoupling Of Currents In Traveling Wave Induction Heating", Journal of Electromagnetic Analysis and Applications, 6: 193-202.
6. Ali K. Al-shaikhli, Abdul-Rahim T. Humod, Fadhil Abbas, 2015. "Closed and quasi-closed yoke configurations for travelling wave induction heaters", IET the Journal of Engineering, pp: 7, DOI: 10.1049/joe.2015.0147.
7. Junhua Wang, S.L. Ho, W.N. Fu, Y.H. Wang, 2010. "Design and Analysis of a Novel Traveling Wave Induction Heating System With Magnetic Slot Wedges for Heating Moving Thin Strips," IEEE Transactions on Magnetic, 46(6): 2175-2178.

8. Bianchi, N., F. Dughiero, 1995. "Optimal design techniques applied to transverse-flux induction heating systems," IEEE Transactions on in Magnetics, 31(3): 1992-1995.
9. Youhua Wang, Junhua Wang, S.L. Ho, Lingling Pang and W.N. Fu, 2011. "A neural network combined with a three-dimensional finite-element", Journal of Applied Physics 110, 093907.
10. Carrillo, E., M.A. Barron, J. Gonzalez, 2005. "Modeling of the circuit parameters of an induction device for heating of a nonmagnetic conducting cylinder by means of a traveling wave as an excitation source," Electrical and Electronics Engineering, 2nd International Conference, pp: 258-261.
11. Ho, S.L., Junhua Wang, W.N. Fu, Y.H. Wang, 2009. "A Novel Crossed Traveling Wave Induction Heating System and Finite-Element Analysis of Eddy Current and Temperature Distributions," IEEE Transactions on Magnetics, 45(10): 4777-4780.
12. Lingling Pang, Youhua Wang, and Tanggong Chen, 2010. "New Development of Traveling Wave Induction Heating", IEEE Transactions On Applied Superconductivity, 20(3).